

Synchronous intracrystalline $\delta^{13}\text{C}$ and $\delta^{18}\text{O}$ differences in natural calcite crystals

J. A. D. DICKSON

Department of Earth Sciences, University of Cambridge, Downing Street, Cambridge CB2 3EQ, UK

Abstract

New intersectorial isotope data are presented for two calcites. Mendip calcite shows no detectable $\delta^{13}\text{C}$ and $\delta^{18}\text{O}$ differences between synchronous {2134} and {0114} sectors. Nottingham calcite shows a $\delta^{13}\text{C}$ difference of 1.0‰ and a $\delta^{18}\text{O}$ difference of 0.5‰ between synchronous {4041} and {0001} sectors. Data now available for 5 different calcites show the magnitude of intersectorial fractionation is variable; the effect on $\delta^{13}\text{C}$ is twice that on $\delta^{18}\text{O}$. All five natural calcites also show erratic isotopic differences between symmetrically-equivalent synchronous sectors. Intersectorial isotopic fractionation is probably widespread but its cause and quantification require further work. Synchronous intracrystalline isotopic differences should be accommodated in the interpretation of isotopic data and should influence future sampling strategy.

KEYWORDS: calcite, oxygen isotopes, carbon isotopes.

Introduction

NATURAL or synthetic, abiotic calcite crystals can show a variety of internal zonal patterns (Reeder, 1991). These patterns can be divided into two categories: (1) Zones caused by sequential change in composition; zonal boundaries are parallel to the growth surface — exemplified by mantle and oscillatory zoning; (2) Zones caused by simultaneous changes in composition; zonal boundaries are discordant to the growth surface — exemplified by sector zoning. Calcite crystals used in this study show a combination of both types of zoning. Synchronous changes in composition were monitored along mantle or oscillatory zones traced across sector zone boundaries. The zonal patterns were displayed using stains or cathodoluminescence. Intracrystalline compositional differences in calcite have been recorded for cations Fe^{2+} , Mn^{2+} , Mg^{2+} and Sr^{2+} (Reeder and Grams, 1987; Hendry and Marshall, 1991; and others) for anions SO_4^{2-} and SeO_4^{2-} (Staudt *et al.*, 1994; and Reeder *et al.*, 1994).

Interpretation of stable isotope data from calcite relies on a complete knowledge of fractionation behaviour, yet intracrystalline effects are rarely considered. Intersectorial differences in stable

carbon and oxygen isotopes from calcite has been noted by Dickson (1991) but is disclaimed by Klein and Lohmann (1995). This paper reports analyses on new calcite samples that contribute new and useful observations regarding intracrystalline differences of $\delta^{13}\text{C}$ and $\delta^{18}\text{O}$ in calcite.

Methods and materials

Two samples of natural calcite which show internal elemental zoning were selected for analysis. A series of analyses were taken from different sectors along or between growth zones, so the set of analyses belong to one time interval of growth. The two samples display crystal faces that were identified and indexed by goniometry (Miller-Bravais notation based on the hexagonal cell is used; older works use the same notation but based on the morphological cell).

Mendip calcite consists of elongate (80mm long) crystals from a sulphide-bearing vein that cuts Carboniferous Limestone of the Mendip Hills, Chipping Sodbury, United Kingdom. The dilational vein is partly filled by calcite crystals which seeded on both walls and enlarged as they grew towards each other. The crystals from opposite walls did not meet, but line a central void with dog-tooth terminations —

a combination of $\{2\bar{1}\bar{3}4\}$ scalenohedral and $\{01\bar{1}4\}$ rhombohedral faces. A single crystal from a thin section cut at right angles to the crystal's *c*-axis and parallel to the vein wall was used for sampling. The section was stained (Dickson, 1965) to reveal many mantle zones divided into $\{2\bar{1}\bar{3}4\}$ and $\{01\bar{1}4\}$ sectors; sectors are labelled by the indices of the faces under which they grew in Fig. 1. The identity of the internal faces was determined by stereographic projection of interfacial angles and computer modelling. Sampling was done with a steel needle, extracting powder from the thin section under a binocular microscope. All calcite from the thin section (40 μm thick) between mantle zone boundaries was removed around the crystal. Zonal boundaries were imaged only on the section's upper surface which introduces a sampling error for inclined zones. This error depends on the zone's inclination to the section surface and the width of sample trench (measured parallel to growth direction). The $\{01\bar{1}4\}$ faces of the Mendip calcite are inclined at $44\frac{1}{2}^\circ$ to the *c*-axis; the $\{2\bar{1}\bar{3}4\}$ faces at 69° . The narrowest trench width used (greatest error) was 200 μm , the trench depth was 40 μm deep, introducing a 20% (by volume) error for $\{01\bar{1}4\}$ faces and a 6½% error for $\{2\bar{1}\bar{3}4\}$ faces. Different

sectors in the same mantle zone have different widths (Fig. 1) which may be due to differing angles of intersection with the plane of the thin section and/or differing growth rates.

Nottingham calcite consists of a single crystal broken from a sheet of crystals that nucleated on a flat substrate and enlarged as they grew away from that substrate (Nottingham University Geology Collection #11418). All crystals in the sheet are similarly terminated by $\{4041\}$ acute rhombohedral faces capped by a single $\{0001\}$ basal pinacoid (Fig. 2). Powder was scraped for analysis from the surfaces of seven external faces. A thin section cut parallel to the *c*-axis of the Nottingham calcite exhibited oscillatory and sector zoning using a cathodoluminescence (CL) microscope. The internal oscillatory zones lie parallel to the external crystal faces. The same sampling procedure as used for the Mendip calcite was employed on the thin section of Nottingham calcite except zonal position was judged from CL photographs. After sampling, the location of pits in the thin section was checked by re-examination in the CL microscope. The distance between any two consecutive oscillatory zones, when traced from the $\{4041\}$ sector across sector boundaries, double in thickness across the $\{0001\}$

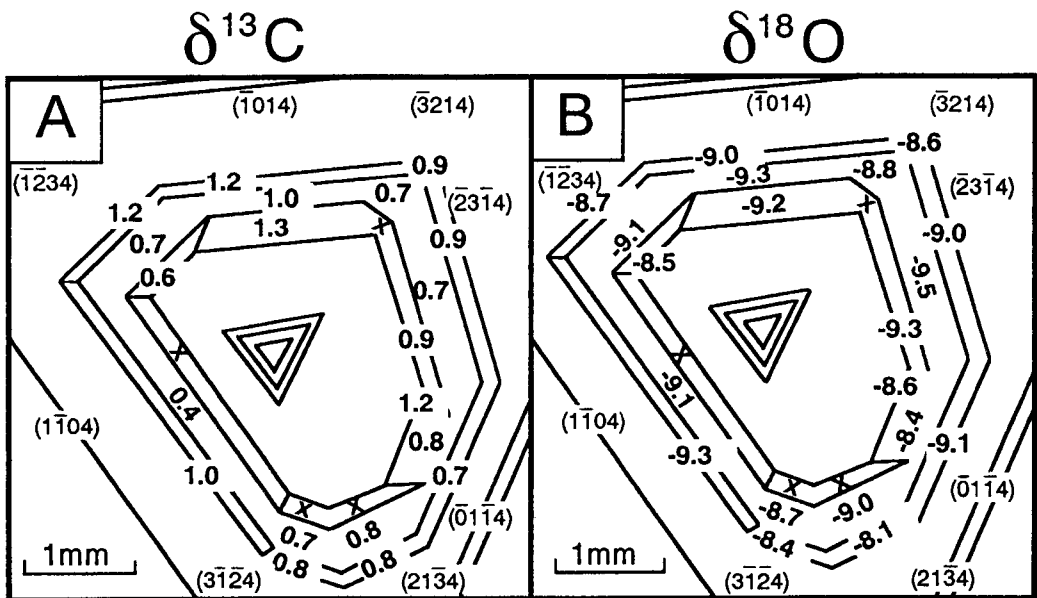


FIG. 1. Pattern of mantle zoning shown by staining thin section through a single crystal of Mendip calcite. Three synchronous mantle zones are subdivided into 8 sectors. Each sector is related to the crystal face under which it grew and are indexed. A. shows $\delta^{13}\text{C}$ VPDB data plotted over sample locations; B. shows $\delta^{18}\text{O}$ VPDB data plotted over sample locations. Data tabulated in Table 1.

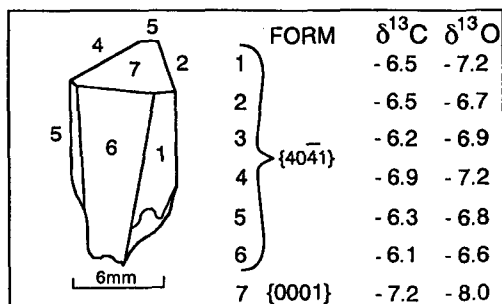


FIG. 2. Sketch showing external crystal faces of a Nottingham calcite crystal. Seven faces numbered and stable isotope data listed for analyses of powder scraped from each face.

sector (Figs. 3 and 4). The thin section is cut parallel to the growth direction of the {0001} sector and at a slight angle to the $\{40\bar{4}1\}$ sector thus the {0001} sector grew at least twice as fast as the $\{40\bar{4}1\}$ sectors.

The calcite powder analysed was routinely baked at 425°C under vacuum to decompose any organic contamination. The samples were then reacted with 100% orthophosphoric acid at 90°C using a V.G. Isotech Isocarb common acid bath system, and the carbon dioxide evolved analysed in a V.G. Isotech PRISM mass spectrometer. The results were calibrated to VPDB using data from repeated analysis of a carbonate standard. Analytical precision is better than 0.08‰.



FIG. 4. Cathodoluminescence micrograph of Nottingham calcite section. Inclined sector boundary separates horizontal {0001} pinacoid face from sub-vertical $\{41\bar{4}1\}$ rhombohedral face. A multitude of fine oscillatory zones can be traced through both sectors.

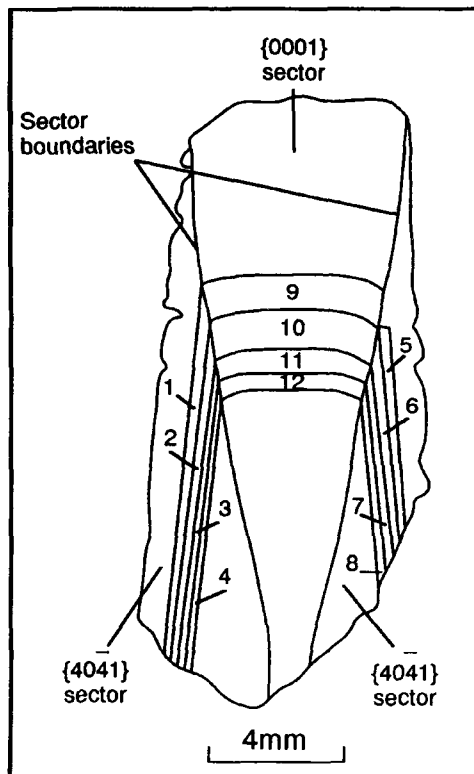


FIG. 3. Line diagram of thin section cut parallel to c -axis of Nottingham calcite crystal. Position of 5 oscillatory zones and 2 sector boundaries as revealed by CL are shown. Sample numbers for 4 consecutive mantle zones each divided into two inclined $\{40\bar{4}1\}$ and one horizontal {0001} sector marked, see Table 2. Box shows area of Fig. 4.

Results

Stable isotope data for Mendip calcite from three consecutive mantle zones, each subdivided into 8 sectors, are given in Fig. 1 and Table 1. Consistent differences between non-equivalent sectors in $\delta^{13}\text{C}$ and $\delta^{18}\text{O}$ ratios are not indicated by these data. It might be expected that data from different equivalent sectors of the same mantle zone should show little variation but this is untrue. The outer mantle zone of the Mendip calcite shows $\delta^{13}\text{C}$ variations of 0.4‰ between $\{21\bar{3}4\}$ sectors and 0.6‰ between $\{10\bar{1}4\}$ sectors, and $\delta^{18}\text{O}$ variations of 0.2‰ between $\{10\bar{1}4\}$ sectors and 0.9‰ between $\{21\bar{3}4\}$ sectors. Stable isotope data for the Nottingham calcite from four internal mantle zones, each subdivided into three

TABLE 1. Stable isotope data calibrated to VPDB, Mendip calcite, determined for three consecutive mantle zones (rows) each divided into 8 sectors (columns)

Sector	(21 $\bar{3}$ 4)	(3 $\bar{1}$ $\bar{2}$ 4)	(1 $\bar{1}$ 04)	($\bar{1}$ $\bar{2}$ 34)	($\bar{1}$ 014)	($\bar{3}$ 214)	($\bar{2}$ 3 $\bar{1}$ 4)	($\bar{0}$ 1 $\bar{1}$ 4)
$\delta^{13}\text{C}$	Time ↑ 0.8	0.8	1.0	1.2	1.3	0.9	0.9	0.7
	0.8	0.7	0.4	0.7	1.0	0.7	0.7	0.8
	x	x	x	0.6	1.2	x	0.9	1.2
$\delta^{18}\text{O}$	Time ↑ -8.1	-8.4	-9.3	-8.5	-9.2	-8.6	-9.0	-9.1
	-9.0	-8.7	-9.1	-9.1	-9.3	-8.8	-9.5	-8.4
	x	x	x	-8.7	-9.0	x	-9.3	-8.6

sectors are given in Fig. 3 and Table 2. The $\delta^{13}\text{C}$ data show consistent differences between {40 $\bar{4}$ 1} and {0001} sectors, mean $\delta^{13}\text{C}$ for {40 $\bar{4}$ 1} sectors = -6.4‰, mean $\delta^{13}\text{C}$ for {0001} sector = -7.4‰. The $\delta^{18}\text{O}$ data are more variable and probably indicate a small intersectorial difference; mean $\delta^{18}\text{O}$ for {40 $\bar{4}$ 1} sectors = -1.4‰, mean $\delta^{18}\text{O}$ for {0001} sectors = -1.9‰. The behaviour of $\delta^{13}\text{C}$ and $\delta^{18}\text{O}$ in the Nottingham internal data differs: carbon remains constant through time, with a constant difference between non-equivalent sectors (Table 2). The oxygen data varies with time (between mantle zones 4 to 1) by ~4‰ for the three sectors analysed. Considerable synchronous variation also exists between the two {40 $\bar{4}$ 1} sectors: mantle zone 1 = +0.6‰; mantle zone 3 = -0.5‰. The $\delta^{18}\text{O}$ values for the {0001} sector are generally higher (less than 1‰) than the two time-equivalent {40 $\bar{4}$ 1} sectors. However, the data show considerable scatter and inconsistency. This may either be due to errors in sample position (exacerbated by the rapid temporal variation of $\delta^{18}\text{O}$ in the Nottingham calcite) or to

$\delta^{18}\text{O}$ intrasectorial variations, in an analogous manner to those reported for cation variations in calcite by Paquette and Reeder (1995). Data for the Nottingham calcite derived from the terminal faces show a similar pattern of differences to the internal data. $\delta^{13}\text{C}$ values are similar to the internal analyses but $\delta^{18}\text{O}$ from the surface samples has changed and are depleted in $\delta^{18}\text{O}$ relative to the internal data. The intersectorial difference in $\delta^{18}\text{O}$ for the terminal faces is more marked than for the internal data (Fig. 2).

Discussion

The frequency with which intersectorial isotope variation affects natural calcite is unknown. Its occurrence in many samples cannot be determined because crystal size is too small to be analysed. This situation is likely to remain unchanged for micrites. However, much existing stable isotope data has been convincingly interpreted using existing fractionation factors. This implies either intersectorial differences are unimportant or these effects go unrecognised because bulk sampling (even one crystal) homogenises these variations so they cannot be identified.

Technological advances in mass spectrometry that will allow smaller samples to be analysed will have two effects: (1) intersectorial variations can be investigated in smaller crystals, and (2) smaller-scale variations in large crystals can be examined. It is known that Sr^{2+} and Mn^{2+} vary in concentration along single crystal faces, termed intrasectorial zoning by Paquette and Reeder (1990). This type of intrafacial variation has been called on to explain isotopic fluctuations in data collected from synchronous sectors in calcite by Klein and Lohmann (1995) and in quartz by Onasch and Vennemann (1995).

Intersectorial isotopic differences have been investigated on mm-sized crystals so crystallographic planes can be directly identified. However crystallographic orientation can sometimes be inferred when preferred growth along a single fixed direction

TABLE 2. Stable isotope data calibrated to VPDB, Nottingham calcite. Determined for 12 numbered locations on thin section, Fig. 3. Four consecutive mantle zones each divided into two {40 $\bar{4}$ 1} sectors and one {0001} sector

Sector	{40 $\bar{4}$ 1}	{0001}	{40 $\bar{4}$ 1}
$\delta^{13}\text{C}$	Time ↑ 1 -6.2	9 -7.1	5 -6.3
	2 -6.4	10 -7.5	6 -6.4
	3 -6.5	11 -7.3	7 -6.6
	4 -6.4	12 -7.6	8 -6.6
$\delta^{18}\text{O}$	Time ↑ 1 +1.1	9 +1.4	5 +1.7
	2 -0.4	10 -0.6	6 -0.3
	3 -3.0	11 -3.7	7 -2.5
	4 -3.7	12 -4.5	8 -3.8

TABLE 3. Comparison of data collected from calcites analysed for intersectorial isotopic effects. Figures beneath $\delta^{13}\text{C}$ and $\delta^{18}\text{O}$ are differences in means for sections shown. Stable isotope data for Bonsall Moor calcite may have biased results due to surface sampling (Dickson, 1995)

Calcite type	Forms present	T°C	Elements detected	Intersectorial effect
El Paso Klien and Lohmann, 1995	{21 $\bar{3}$ 4} {23 $\bar{1}$ 4} {01 $\bar{1}$ 8}	$\leq 125^\circ\text{C}$	Fe Mn Sr Mg	{21 $\bar{3}$ 4} none {01 $\bar{1}$ 8}
Mendip Dickson, this paper	{21 $\bar{3}$ 4} {01 $\bar{1}$ 4}	hydrothermal	Fe Mn	{21 $\bar{3}$ 4} Fe Mn {01 $\bar{1}$ 4} no isotopic differences
Bonsall Moor	{21 $\bar{3}$ 4} {01 $\bar{1}$ 4} {2.9.11.20}	hydrothermal	Fe Mn	Fe Mn {21 $\bar{3}$ 4} $\delta^{13}\text{C}$ $\delta^{18}\text{O}$ {01 $\bar{1}$ 4} 2.2‰ 0.9‰
Nottingham Dickson, this paper	{40 $\bar{4}$ 1} {0001}	?	Mn no Fe	Mn {40 $\bar{4}$ 1} $\delta^{13}\text{C}$ $\delta^{18}\text{O}$ {0001} 1.0‰ 0.5‰
Abercriban Dickson (1991)	?	Meteoric	Fe Mn	Fe Mn ? $\delta^{13}\text{C}$ $\delta^{18}\text{O}$? 0.6‰ 0.1‰

occurs. For instance, this is the case with some organically-mediated biominerals where calcification occurs by epitaxy on an organic template (Weiner and Traub, 1984). Lattice orientation of skeletal calcite is fixed for certain taxonomic groups so once this group has been identified skeletal orientation can be inferred, even for the smallest crystals. This constancy of orientation in some skeletal secretions, coupled with surface effects and growth mechanisms on the mineralising surface, may cause isotopic differences that are directly analogous to intersectorial isotopic differences. This process, if it does

occur, can be one element of the 'vital' effect, a loose term applied to disequilibrium in biogenic precipitates.

The five zoned natural calcite crystals that have been investigated for intersectorial differences in $\delta^{13}\text{C}$ and $\delta^{18}\text{O}$ show variable properties, Table 3. Although the magnitude of intersectorial differences varies from undetectable to $>2\%$ for $\delta^{13}\text{C}$, when they do occur carbon is affected twice as much as oxygen. It is interesting to note that some synthetic (Turner, 1982) and some natural inorganic calcite (Clark *et al.*, 1992) are depleted in ^{13}C and ^{18}O relative to a

TABLE 4. Comparison of data collected from quartz analysed for intersectorial effects

Quartz type	Form present	T°C	Intersectorial effects
Amethyst Klemm <i>et al.</i> , 1990	{10 $\bar{1}$ 0} {10 $\bar{1}$ 1} {01 $\bar{1}$ 1}	?	{10 $\bar{1}$ 0} $\delta^{18}\text{O} = 0.4\%$ {10 $\bar{1}$ 1} {10 $\bar{1}$ 1} $\delta^{18}\text{O} = 0.2\%$ {01 $\bar{1}$ 1}
Smoky Klemm <i>et al.</i> , 1991, 1992	{10 $\bar{1}$ 0} {10 $\bar{1}$ 1}		{10 $\bar{1}$ 0} $\delta^{18}\text{O} = 0.42\%$ {10 $\bar{1}$ 1}
Molas Lake Onasch and Vennemann, 1995	?	245°C	? $\delta^{18}\text{O} = 0.2\%$?

predicted equilibrium value (with carbon exhibiting twice the deviation of oxygen). This deviation, in both cases, is related to kinetic effects. The isotope data from all five natural calcites investigated for intersectorial differences also show a different type of variation. Data from synchronous, symmetrically-equivalent sectors show inconsistent values; the variation is usually less than 1‰ but above analytical error. These variations have been homologised with intrasectorial zonation of trace ions but a satisfactory explanation for these erratic variations in stoichiometric components of calcite is wanting. Three natural quartz crystals analysed exhibit similar isotopic variations (Table 4) to calcite. A fuller understanding of intercrystalline isotopic variation in natural calcite will be assisted by additional data, including conditions of precipitation, but even more useful will be investigations into synthetic calcite where the whole system can be monitored. The means of growing sector-zoned calcite crystals of sufficient size (Gruzensky, 1967; Paquette and Reeder, 1990) for such investigations is already known.

Acknowledgements

Stable isotope analyses were performed by Mike Hall, Godwin Laboratory, Cambridge. Thanks go to Dr R.J. Reeder whose review considerably improved this paper.

References

- Clark, I.D., Fontes, J.C. and Fritz, P. (1992) Stable isotope disequilibria in travertine from high pH waters: Laboratory investigations and field observations from Oman. *Geochim. Cosmochim. Acta*, **56**, 2041–50.
- Dickson, J.A.D. (1965) A modified staining technique for carbonates in thin section. *Nature*, **205**, 587.
- Dickson, J.A.D. (1991) Disequilibrium carbon and oxygen isotope variations in natural calcite. *Nature*, **353**, 842–4.
- Dickson, J.A.D. (1995) Isotopic homogeneity among nonequivalent sectors of calcite: comment. *Geology*, **24**, 95.
- Gruzensky, P.M. (1967) Growth of calcite crystals. In *Crystal growth* (H.S. Peiser, ed.). Pergamon, 367–87.
- Hendry, J.P. and Marshall, J.D. (1991) Interpretation of complex non-concentric zoning fabrics in sparry calcite cements: Middle Jurassic limestones, central England. *Sedimentary Geology*, **75**, 39–55.
- Klein, R.T. and Lohmann, K.C. (1995) Isotopic homogeneity among nonequivalent sector of calcite. *Geology*, **23**, 633–6.
- Klemm, A., Banerjee, A. and Hoernes, S. (1990) A new intracrystalline isotope effect: $\delta^{18}\text{O}$ under the faces of amethyst. *Zeitschrift für Naturforschung*, **45a**, 1374–6.
- Klemm, A., Banerjee, A. and Hoernes, S. (1991) Fractionation of oxygen isotopes at the faces of smoky quartz. *Zeitschrift für Naturforschung*, **46a**, 1133–4.
- Klemm, A., Banerjee, A. and Hoernes, S. (1992) Further study of intersectorial isotopes fractionation in quartz. *Zeitschrift für Naturforschung*, **47a**, 1232–4.
- Onasch, C.M. and Vennemann, T.W. (1995) Disequilibrium partitioning of oxygen isotopes associated with sector zoning in quartz. *Geology*, **23**, 1103–6.
- Paquette, J. and Reeder, R.J. (1990) New types of compositional zoning in calcite: Insights into crystal-growth mechanisms. *Geology*, **58**, 1244–7.
- Paquette, J. and Reeder, R.J. (1995) Relationship between surface structure, growth mechanism, and trace element in corporation in calcite. *Geochim. Cosmochim. Acta*, **59**, 735–49.
- Reeder, R.J. (1991) An overview of zoning in carbonate minerals. In *Luminescence Microscopy, Quantitative and qualitative aspects* (C.E. Barker and O.C. Kopp, eds). Society of Economic Paleontologists and Mineralogists: Short Course Notes, **25**, 77–82.
- Reeder, R.J. and Grams, J.C. (1987) Sector zoning in calcite cement crystals: Implications for trace element distributions in carbonates. *Geochim. Cosmochim. Acta*, **51**, 187–94.
- Reeder, R.J., Lamble, G.M., Lee, J.F. and Staudt, W.J. (1994) Mechanism of SeO_4^{2-} substitution in calcite; an XAFS study. *Geochim. Cosmochim. Acta*, **58**, 5639–46.
- Staudt, W.J., Reeder, R.J. and Schoonen, M.A.A. (1994) Surface structural controls on compositional zoning of SO_4^{2-} and SeO_4^{2-} in synthetic calcite single crystals. *Geochim. Cosmochim. Acta*, **58**, 2087–98.
- Turner, J.V. (1982) Kinetic fractionation of carbon-13 during calcium carbonate precipitation. *Geochim. Cosmochim. Acta*, **46**, 1183–91.
- Weiner, S. and Traub, W. (1984) Macromolecules in mollusc shells and their function in biomineralization. *Phil. Trans. Roy. Soc. London B*, **304**, 425–34.

[Manuscript received 20 April 1996;
revised 31 July 1996]